Bioorganic & Medicinal Chemistry Letters 19 (2009) 2735–2738

Contents lists available at ScienceDirect

Bioorganic & Medicinal Chemistry Letters

journal homepage: www.elsevier.com/locate/bmcl

Identification of pyrazolo[1,5-*a*]pyrimidine-3-carboxylates as B-Raf kinase inhibitors

Ariamala Gopalsamy [a,*], Greg Ciszewski [a], Yongbo Hu [a], Frederick Lee [a], Larry Feldberg [b], Eileen Frommer [b], Steven Kim [b], Karen Collins [b], Donald Wojciechowicz [b], Robert Mallon [b]

[a] *Chemical and Screening Sciences, Wyeth Research, 401 N. Middletown Road., Pearl River, NY 10965, USA*
[b] *Discovery Oncology, Wyeth Research, 401 N. Middletown Road, Pearl River, NY 10965, USA*

ARTICLE INFO

Article history:
Received 13 February 2009
Revised 20 March 2009
Accepted 25 March 2009
Available online 28 March 2009

Keywords:
B-Raf
B-Raf Inhibitor
Pyrazolo[1,5-*a*]pyrimidine-3-carboxylate

ABSTRACT

B-Raf kinase plays a critical role in the Raf-MEK-ERK signaling pathway and inhibitors of B-Raf could be used in the treatment of melanomas, colorectal cancer, and other Ras related human cancers. We have identified novel small molecule pyrazolo[1,5-*a*]pyrimidine derivatives as B-Raf kinase inhibitors. Structure–activity relationship was generated for various regions of the scaffold to improve the biochemical profile.

© 2009 Elsevier Ltd. All rights reserved.

Raf kinases are serine/threonine protein kinases. They play central role in cell growth and survival and are components of Raf-MEK-ERK signaling pathway.[1] This pathway normally mediates cellular responses to growth signals, however, Ras mutations that are associated with 30% of all cancers constitutively activate this pathway. Of the three Raf human isoforms (A-, B- and C-), activating B-Raf mutations have been found in 66% of malignant melanomas[2] and in a smaller fraction of other cancers including those of the colorectum. The most common B-Raf mutation is valine substitution by glutamic acid at amino acid position (V600E). B-Raf mutations in these cancers were found in a systematic genome-wide screening effort to detect alterations in genes that control cell proliferation, differentiation, and death. Inhibitors of B-Raf could be used in the treatment of melanomas, colorectal cancer, and other Ras related human cancers thus making B-Raf kinase a compelling drug discovery target.

A number of small molecule inhibitors of B-Raf have emerged in the recent past[3] including the most intensively studied Sorafenib,[4] triarylimidazole SB-590885[5] and azaindole PLX-4720[6] (Fig. 1). As part of our on-going effort to identify B-Raf inhibitors, we established an HTS assay to monitor the kinase activity of both wt and mutant (V600E) forms of this protein. This assay was an adaptation of our previously described assay system to detect inhibitors of both C-Raf and MEK1 kinases.[7] Briefly, B-Raf was used to phosphorylate GST-tagged inactive MEK1. MEK1 phosphorylation was measured by a phospho-specific antibody that detected B-Raf phosphorylation of the two serine residues at positions 217 and 221 on MEK1.[8] From this effort pyrazolo[1,5-*a*]pyrimidine-3-carboxylate **1** (Fig. 2) was identified as a promising B-Raf kinase inhibitor.

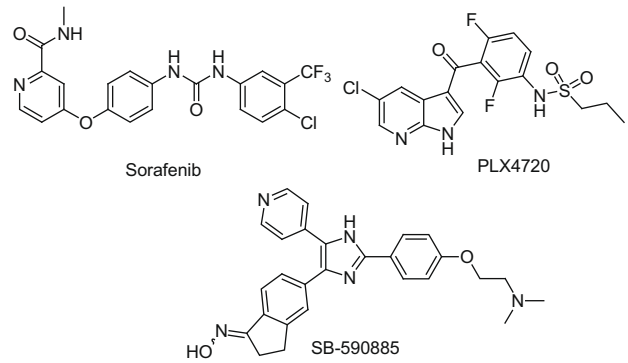

Figure 1. Examples of B-Raf kinase inhibitors.

Compound **1** showed an IC50 of 1.5 μM in the B-Raf kinase assay. It inhibited the growth of a variety of tumor cell lines including BXPC-3 (IC_{50}: 3.25 μM), HT29 (IC_{50}: 7.0 μM), A375 (IC_{50}: 3.8 μM), SW620 (IC_{50}: 8.3 μM), LOVO (IC_{50}: 3.87 μM), WM266-4 (IC_{50}: 6.2 μM) and CaCo-2 (IC_{50}: 6.6 μM). It is a novel scaffold for B-Raf kinase inhibition. This compound was found to be selective when tested against a panel of kinases including PDK-1, m-TOR, Tpl2,

* Corresponding author.
E-mail address: gopalsa@wyeth.com (A. Gopalsamy).

0960-894X/$ - see front matter © 2009 Elsevier Ltd. All rights reserved.
doi:10.1016/j.bmcl.2009.03.129

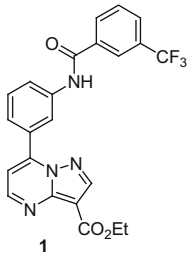

Figure 2. B-Raf inhibitor hit **1** (pyrazolo[1,5-*a*]pyrimidine-3-carboxylate) identified from high through-put screen.

BTK, AKT, CDK-4, LCK, LYN, KDR, IGFR-1, SRC and PI3 Kα (IC_{50} > 10 μM). The key structural features of the compound had high degree of resemblance to the reported B-Raf kinase inhibitor Sorafenib. A docking study was performed with the standard Glide2.0 SP procedure, using the crystal structure of Sorafenib_B-Raf complex.[9] Illustrated in Figure 3 is a binding model of compound **1** in complex with B-Raf. The model indicated that the amide of compound **1** makes two hydrogen bonds to the enzyme: one to the side chain of Glu500 and another to the backbone NH of Asp593. No specific polar interaction was found between the ester moiety and B-Raf, but the ester does make hydrophobic interactions with Ile462, Trp530 and Phe582 with the ethyl group pointing toward a solvent accessible region. On the other end of the molecule, the aromatic ring of the amide region sits at a hydrophobic pocket which consists of Ile 512, His 573 and Ile 571. The ring is partially exposed to solvent at the C4 position. Based on this information, the initial structure–activity relationship for the ester moiety, amide linker and the aromatic ring of the amide region were explored.

The analogs designed to obtain structure–activity relationship were synthesized by following the synthetic sequence employed for compound **1** as shown in Scheme 1.[10] Reaction of 3-nitroacetophenone **2** with *N*,*N*-dimethylformamidedimethylacetal followed by condensation with 5-aminopyrazole-4-carboxylate **4** afforded ester **5**. Selective reduction of the nitro group of compound **5** afforded the key intermediate aniline **6** which was further derivatized to the required amides by reacting with appropriate acid chlorides. Reacting the common intermediate amine **6** with various isocyanates or triphosgene and appropriate amines generated urea analogs. Pyrazolo[1,5-*a*]pyrimidine-3-carboxylic acid **8** and carboxamides **9** were prepared starting from the ester **1**, which was hydrolyzed to the acid and coupled with different amines (Scheme 2).

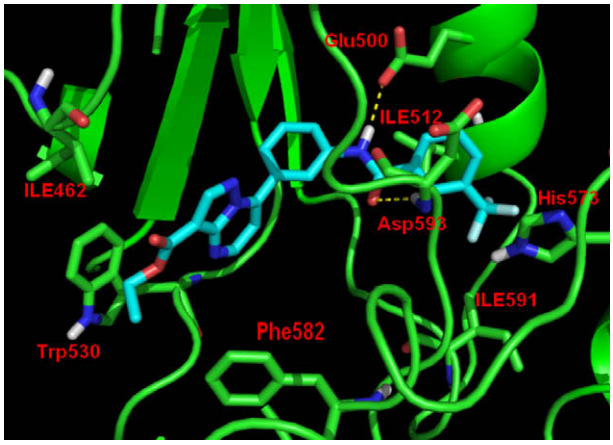

Figure 3. Docked conformation of compound **1** in the active site of B-Raf.

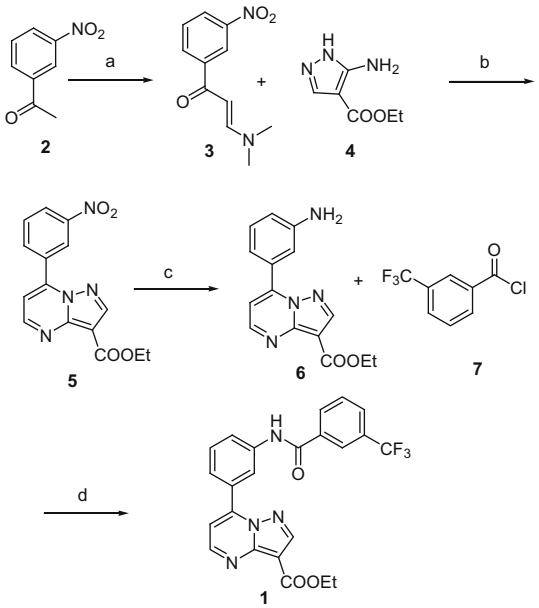

Scheme 1. Reagents and conditions: (a) DMF–DMA, reflux, 18 h, 79%; (b) acetic acid, 80 °C, 12 h, 72%; (c) Fe, acetic acid, 80 °C, 3 h, 60%; (d) pyridine, rt, 70%.

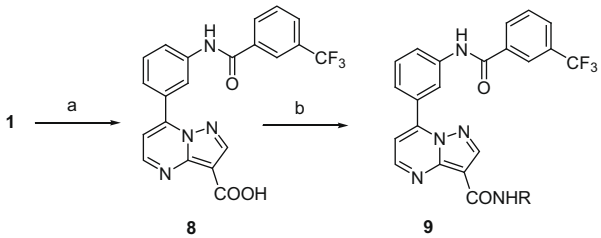

Scheme 2. Reagents and conditions: (a) 2 M LiOH, THF–MeOH, 40 °C, 6 h, 90%; (b) RNH_2, PYBOP, DIEA, DMF, rt, 12 h.

Initial understanding of the SAR was directed towards determining the importance of the trifluoromethyl group and its position on the aromatic ring (Table 1) while maintaining the rest of the molecule intact. Elimination of the group resulted in an unsubstituted phenyl analog **10** with significantly reduced activity. Replacing the CF_3 group with other substituents was also attempted. Both electron withdrawing groups and electron releasing groups were introduced to probe the electronic effects. Most of the aromatic substituents including halogens were not favorable. However, introduction of trifluoromethoxy group (compound **16**) maintained the activity indicating that the lipophilicity of the group is probably more important than the electronics for binding interactions as indicated by our docking studies. Moving the CF_3 group from *meta* position of the aromatic ring (R^2) to the *para* position (R^3) reduced the activity as shown by analog **17**.

Having established the requirement of a lipophilic group like CF_3 in the R^2 position of the aromatic ring, we explored the tolerance of an additional substituent in that ring as shown by analogs **18**–**22** in Table 1. Introduction of a small group like methyl, methoxy and chloro in the R^3 position along with CF_3 group in the R^2 position of the aromatic ring was very well tolerated (compounds 18–20). However, moving these substituents to the R_5 position of the aromatic ring in the presence of the CF_3 group in the R^2 position (compound **21** and **22**) was not favorable. This is probably due to the steric hindrance introduced by these groups around the amide linker which forms two key hydrogen bond interactions

Table 1
B-Raf kinase activity of pyrazolopyrimidine analogs

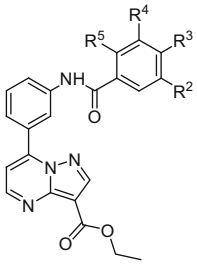

Compd	R^2	R^3	R^4	R^5	B-Raf kinase IC_{50}[a] (μM)
1	CF_3	H	H	H	1.54
10	H	H	H	H	>10
11	CH_3	H	H	H	>10
12	OCH_3	H	H	H	>10
13	Cl	H	H	H	>10
14	Br	H	H	H	>10
15	CN	H	H	H	>10
16	OCF_3	H	H	H	1.57
17	H	CF_3	H	H	>10
18	CF_3	CH_3	H	H	0.5
19	CF_3	OCH_3	H	H	1.03
20	CF_3	Cl	H	H	4.27
21	CF_3	H	H	CH_3	>10
22	CF_3	H	H	Cl	>10

[a] Values are means of two or more experiments.

with the enzyme. Replacing the entire aromatic group with aliphatic groups like methyl or neopentyl was not encouraging. Similarly replacing the *m*-trifluoromethylphenyl ring with *m*-trifluoromethylbenzyl ring was not accommodated. Replacing with hetroaromatics like thiophene or pyridyl rings resulted in loss of activity.

As predicted by our proposed binding of compound **1** to the enzyme, SAR for the amide linker variation indicated that the reverse amide and sulfonamides are not ideal. However, the analogs with urea linker which maintains the required hydrogen bond interactions, showed slight increase in potency as shown in Table 2. As observed in the case of amide linkers, moving the CF_3 group to *ortho* or *para* position was not beneficial. A similar effect was observed with CF_3 replacement with other substituents like chloro (compound **26**). Additional substituents in the R^3 position provided slight increase in activity in the urea analogs as well, as shown by compounds **27**-**29** (Table 2). From our docking studies, this observed conservation of SAR for the hydrophobic region is explained by the movement of the protein residues in the binding pocket to accommodate the longer urea linker.

Table 2
SAR for amide linker modification

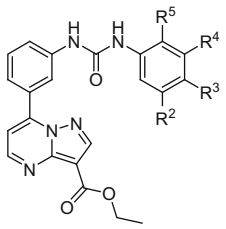

Compd	R^2	R^3	R^4	R^5	B-Raf kinase IC_{50}[a] (μM)
23	CF_3	H	H	H	0.54
24	H	CF_3	H	H	3.6
25	H	H	H	CF_3	>10
26	Cl	H	H	H	>10
27	CF_3	CH_3	H	H	0.36
28	CF_3	Cl	H	H	0.36
29	CF_3	F	H	H	0.24
30	CF_3	H	H	Cl	>10

[a] Values are means of two or more experiments.

Table 3
SAR for ester modification

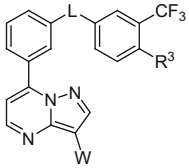

Compd	LINKER (L)	R^3	W	B-Raf kinase IC_{50}[a] (μM)
31	–NH–CO–	H	H	>10
32	–NH–CO–	H	CN	>10
8	–NH–CO–	H	COOH	>10
33	–NH–CO–	H	COOMe	0.41
34	–NH–CO–	H	$COOCH_2CF_3$	1.45
35	–NH–CO–	H	$COOCH_2CH_2N(CH_3)_2$	7.07
36	–NH–CO–	H	$CONH_2$	>10
37	–NH–CO–	H	$CONHCH_3$	>10
38	–NH–CO–	H	$CONHCH_2CH_2N(CH_3)_2$	5.88
39	–NH–CO–	H	$CONHCH_2CH_2$–N–morpholinyl	6.34
40	–NH–CO–NH–	Cl	$CONHCH_2CH_2N(Et)_2$	0.17
41	–NH–CO–NH–	Cl	$CONH(CH_2)_3OCH_3$	0.27
42	–NH–CO–NH–	Cl	$CONHCH_2CH_2$-N-morpholinyl	0.16

[a] Values are means of two or more experiments.

In order to determine the importance of the ethyl ester group in the hit, modifications were attempted at this region (Table 3). Substituting the ethyl ester with other esters (compounds **33**–**35**) maintained the activity. However removal of the ester (analog **31**) or replacing the ethyl ester with acid **8** or nitrile **32** or unsubstituted amide **36** rendered the compounds less active. Since in our proposed binding pose the ethyl group of the ester is solvent exposed, we explored this region further to introduce water solubilizing groups through the carboxamide. A number of analogs were generated (compounds **37**–**42**) using either amide linker or urea linker. This modification was tolerated and some increase in the enzyme activity was observed for the urea analogs. However this modification did not lead to significant boost in the cell activity.[11] The next phase of this hit to lead optimization process will utilize the observed SAR to improve the pharmaceutical properties to realize significant improvement in cell activity.

In summary, as detailed above pyrazolopyrimidine scaffold identified as B-Raf inhibitor from HTS has been optimized to infer SAR for various regions of the molecule. A lipophilic group in the *meta* position of the aromatic group in the amide region was preferred with tolerance for additional substituents. Of the linkers attempted the urea linker was favorable with slight increase in potency. Replacement of the ester with amides was tolerated with slight increase in enzyme potency and provides a handle for introducing water solubilizing groups to improve the pharmaceutical properties of the scaffold. Our continued efforts to elaborate this scaffold to further improve the overall biological and pharmaceutical profile will be reported in future.

Acknowledgments

The authors thank Dr. John Ellingboe for his support of this work. We also thank discovery analytical chemistry group for analytical data.

References and notes

1. Garnett, M. J.; Marais, R. *Cancer Cell* **2004**, *6*, 313–319.
2. Davies, H.; Bignell, G. R.; Cox, C.; Stephens, P.; Edkins, S.; Clegg, S.; Teague, J.; Woffendin, H.; Garnett, M. J.; Bottomley, W.; Davis, N.; Dicks, E.; Ewing, R.; Floyd, Y.; Gray, K.; Hall, S.; Hawes, R.; Hughes, J.; Kosmidou, V.; Menzies, A.; Mould, C.; Parker, A.; Stevens, C.; Watt, S.; Hooper, S.; Wilson, R.; Jayatilake, H.; Gusterson, B. A.; Cooper, C.; Shipley, J.; Hargrave, D.; Pritchard-Jones, K.; Maitland, N.; Chenevix-Trench, G.; Riggins, G. J.; Bigner, D. D.; Palmieri, G.; Cossu, A.; Flanagan, A.; Nicholson, A.; Ho, J. W. C.; Leung, S. Y.; Yuen, S. T.; Weber, B. L.; Seigler, H. F.; Darrow, T. L.; Paterson, H.; Marais, R.; Marshall, C. J.; Wooster, R.; Stratton, M. R.; Futreal, P. A. *Nature* **2002**, *417*, 949.
3. Li, N.; Batt, D.; Warmuth, M. *Curr. Opin. Invest. Drugs* **2007**, *8*, 452–456.
4. Lowinger, T. B.; Riedl, B.; Dumas, J.; Smith, R. A. *Curr. Pharm. Des.* **2002**, *8*, 2269–2278.
5. King, A. J.; Patrick, D. R.; Batorsky, R. S.; Ho, M. L.; Do, H. T.; Zhang, S. Y.; Kumar, R.; Rusnak, D. W.; Takle, A. K.; Wilson, D. M.; Hugger, E. *Cancer Res.* **2006**, *66*, 11100–11105.
6. Tsai, J.; Lee, J. T.; Wang, W.; Zhang, J.; Cho, H.; Mamo, S.; Bremer, R.; Gillette, S.; Kong, J.; Haass, N. K.; Sproesser, K.; Li, L.; Smalley, K. S. M.; Fong, D.; Zhu, Y-L.; Marimuthu, A.; Nguyen, H.; Lam, B.; Liu, J.; Cheung, I.; Rice, J.; Suzuki, Y.; Luu, C.; Settachatgul, C.; Shellooe, R.; Cantwell, J.; Kim, S-H.; Schlessinger, J.; Zhang, K. Y. J.; West, B. L.; Powell, B.; Habets, G.; Zhang, C.; Ibrahim, P. N.; Hirth, P.; Artis, D. R.; Herlyn, M.; Bollag, G. *Proc. Natl. Acad. Sci.* **2008**, *105*, 3041–3046.
7. Mallon, R.; Feldberg, L. R.; Kim, S. C.; Collins, K.; Wojciechowicz, D.; Hollander, I.; Kovacs, E. D.; Kohler, C. *Anal. Biochem.* **2001**, *294*, 48–56.
8. *B-Raf kinase assay*: Flag/6his-tagged recombinant human B-Raf (from Sf9 insect cells; specific activity ~200 U/ml) was used to phosphorylate human non-active Mek1 (GST tagged from *E. coli*); resultant phospho-MEK1 was measured by a phospho-specific polyclonal Ab from Cell Signaling Technology (#9154). B-Raf assay stock solutions were: assay dilution buffer (ADB) containing 20 mM MOPS, pH 7.2, 25 mM β-glycerol phosphate, 5 mM EGTA, 1 mM sodium orthovanadate, 1 mM dithiothreitol; Magnesium/ATP Cocktail (0.5 mM ATP, 75 mM MgCl2) in ADB; active B-Raf in ADB; non-active GST-MEK1 in ADB; and TBST—Tris (50 mM, pH 7.5), NaCl (150 mM), Tween-20 (0.05%). Kinase assays were carried out in a shaking incubator. The protocol was: in 96 well plate format B-Raf (0.4U/assay) and non-active MEK1 (0.4 μg/assay) were incubated with 0.1 mM ATP/ 15 mM MgCl2 for 60 min at 30 °C. This mixture was transferred to anti-GST Ab (Pharmacia) coated 96 well plates (Nunc), and then incubated for 60 min at 30 °C. Plates were then washed 3× with TBST, and then anti-phospho MEK1 Ab was added with incubation for 60 min at 30 °C. Plates were then washed 3× with TBST, and anti-rabbit Ab/Europium conjugate (Wallac) was added with incubation for 60 min (30 °C). A Wallac (Victor) Plate Reader was used to collect data that was analyzed in excel for single point and IC50 determinations.
9. Wan, P. T.; Garnett, M. J.; Roe, S. M.; Lee, S.; Niculescu-Duvaz, D.; Good, V. M.; Jones, C. M.; Marshall, C. J.; Springer, C. J.; Barford, D.; Marais, R. *Cell* **2004**, *116*, 855–867.
10. For experimental details, see: Gopalsamy, A.; Ciszewski, G. M.; Shi, M.; Berger, D. M.; Torres, N.; Levin, J. I.; Powell, D. W. U.S. Pat. Appl. Publ. 2007; *Chem. Abstr.* **2007**, *147*, 386006.
11. Activity of compound **42** in cell lines—BXPC-3 (IC_{50}: 6.8 μM), A375 (IC_{50}: 6.1 μM), LOVO (IC_{50}: 4.7 μM), and CaCo-2 (IC_{50}: 4.6 μM).